



Science  
Press

Available online at [www.sciencedirect.com](http://www.sciencedirect.com)



ScienceDirect

Trans. Nonferrous Met. Soc. China 28(2018) 169–176

Transactions of  
Nonferrous Metals  
Society of China

[www.tnmsc.cn](http://www.tnmsc.cn)



## Transformation and leaching kinetics of silicon from low-grade nickel laterite ore by pre-roasting and alkaline leaching process

Wen-ning MU<sup>1,2</sup>, Xiu-yuan LU<sup>1</sup>, Fu-hui CUI<sup>3</sup>, Shao-hua LUO<sup>1,2</sup>, Yu-chun ZHAI<sup>3</sup>

1. School of Resources and Materials, Northeastern University at Qinhuangdao, Qinhuangdao 066004, China;
2. Key Laboratory of Resources Cleaner Conversion and Efficient Utilization at Qinhuangdao City, Qinhuangdao 066004, China;
3. School of Metallurgy, Northeastern University, Shenyang 110819, China

Received 14 September 2016; accepted 21 April 2017

**Abstract:** The mineralogical phase transformation of a low-grade nickel laterite ore during pre-roasting process and the extraction of silicon during alkaline leaching process were investigated. The results indicate that the reaction activity of nickel ores is effectively improved by pre-roasting at 650 °C for 2 h, because of the transformation of lizardite into magnesium olivine and protoenstatite. When finely ground ore samples (44–61 µm) pre-roasted firstly react with sodium hydroxide solution (60 g/L) with a solid/liquid ratio of 1:5 at 140 °C for 120 min, the extraction of silicon can reach 89.89%, and the other valuable elements of magnesium, iron and nickel are accumulated in the solid residues. The leaching kinetics of nickel laterite ore can be described successfully by the diffusion through the product layer control model. The activation energy is calculated to be 11.63 kJ/mol and the kinetics equation can be expressed as  $1-3(1-x)^{2/3}+2(1-x)=13.53 \times 10^{-2} \exp[-11.63/(RT)]t$ .

**Key words:** low-grade nickel laterite ore; silicon extraction; mineralogical phase transformation; alkaline leaching kinetics

### 1 Introduction

In recent years, there has been an increasing attention for the development and utilization of nickel laterite ores, along with the rapid growth in stainless steel demand and the gradual depletion of sulfide ore reserves [1,2]. It is calculated that the laterite ore reserves which account for about 70% of the world's land-based nickel resources can be used as the dominant source of nickel [3,4]. However, only 40% of the world's nickel production is from nickel laterite ores currently [5]. The main reasons for limiting the development and utilization of the laterite ores are the economic factors of treating processes. Therefore, developing reasonable, feasible and economic techniques for treating nickel laterite ores has become a very urgent task.

Laterite ore deposits are formed by the chemical weathering of nickeliferous peridotite rock under humid climates [6,7]. Through long weathering processes, Ni<sup>2+</sup>

replaces Mg<sup>2+</sup> and Fe<sup>2+</sup> in the lattice of corresponding silicates and ferric iron oxides, and is closely in conjunction with iron oxide and silicate minerals [8]. The concentration of nickel in an ore-body is very low, and typical nickel content in Chinese laterite ore is less than 1%. The complex mineralogical structure has prevented nickel grade from being preconcentrated by some physical beneficiation means [9,10]. Thus, pyrometallurgical or hydrometallurgical methods are exploited for processing low-grade laterite ores.

The pyrometallurgical techniques including pre-reduction and reductive smelting in electric arc furnaces (EAFs) for production of Fe–Ni alloys are well suited for treating saprolitic laterite ores [11]. The primary disadvantage of these processes is that they require considerable energy expenditure which is two to three times higher than that for treating the sulfide ores [12].

High pressure acid leaching (HPAL), atmospheric (acid) leaching (AL) and heap leaching (HL) are referred as the prevailing technologies for hydrometallurgical

**Foundation item:** Project (2014CB643405) supported by the National Basic Research Program of China; Projects (51204036, 51234009) supported by the National Natural Science Foundation of China; Project (BJ201604) supported by the Program for Top Young Talents of Higher Education Institutions of Hebei Province, China

**Corresponding author:** Wen-ning MU; Tel: +86-335-8057478; E-mail: danae2007@163.com  
DOI: 10.1016/S1003-6326(18)64650-3

processing of laterite ores [13]. However, they are more appropriate for treating limonite ore that has high iron content but low garnierite content. The leach liquor always contains significant concentrations of soluble iron and magnesium or aluminium, and these metal impurities need to be subsequently purified [14–16].

In recent years, ZHAI and MU [17,18] have proposed an approach for treating Chinese nickeliferous laterite ores. In this process, high concentration alkaline or molten sodium hydroxide system, carbonation decomposition and ammonia leaching are used for sequential extracting and separating silicon, magnesium, nickel and iron, so as to realize comprehensive utilization of nickeliferous laterite ores. Contrast with acid leaching methods, this process exhibits numerous advantages such as high reactivity, elimination of  $\text{SO}_2$ , high selectivity and good application prospect. The dosage of alkaline is a key factor for treating laterite ores, which determines the economy and environmental protection of the whole process. However, rare research results on alkaline leaching of laterite ores have been reported so far, and the transformation behavior and control steps of valuable components are necessary to be studied further.

Thus, in this work, a Chinese low-grade nickel laterite ore located in Sichuan Province, China, was used as the raw materials. The pre-roasting of nickel ores was conducted followed by leaching with sodium hydroxide solution to extract silicon element for preparing silica. The process can not only achieve the utilization of silicon element to reduce the discharge of solid waste, but also accumulate magnesium and nickel in the leaching residues as an important secondary source. The mineralogical phase transformation of nickel laterite ore during pre-roasting was studied. The effects of different variables, such as leaching temperature, leaching time, sodium hydroxide concentration, particle size and solid/liquid ratio (w/v) on the extraction of silicon were investigated. Different kinetics models were used to analyze the leaching kinetics of laterite ores to obtain Arrhenius activation energies and kinetics equation.

## 2 Experimental

### 2.1 Materials

A low-grade nickel laterite ore collected from Sichuan Province, China, was selected as the representative ore samples in this study. The ore samples were sieved and divided into four size fractions ranging from 44 to 178  $\mu\text{m}$  using Tyler standard sieve. The chemical analysis of each size fraction conducted by X-ray spectrometer is listed in Table 1. Analytical grade sodium hydroxide was used as the leaching reagent in all experiments.

X-ray diffraction equipment using  $\text{Cu K}\alpha$  radiation

was employed to identify the mineralogical components of ore samples from 10° to 70°. The results in Fig. 1 indicate lizardite ( $\text{Mg}_3\text{Si}_2\text{O}_5(\text{OH})_4$ ) and quartz ( $\text{SiO}_2$ ) as major mineral phases, as well as hematite ( $\text{Fe}_2\text{O}_3$ ) and trevorite ( $\text{NiFe}_2\text{O}_4$ ) as minor phases.

**Table 1** Main chemical compositions of nickel laterite ores at different size fractions

Particle size/ $\mu\text{m}$	Mass fraction/%					
	$\text{SiO}_2$	$\text{MgO}$	$\text{Fe}_2\text{O}_3$	$\text{Al}_2\text{O}_3$	$\text{NiO}$	$\text{Cr}_2\text{O}_3$
150–178	35.66	17.81	29.33	4.94	1.12	0.46
104–124	36.27	17.32	29.46	4.87	1.16	0.43
74–89	36.74	16.44	29.75	4.68	1.15	0.48
44–61	36.29	17.79	29.80	4.82	1.14	0.44

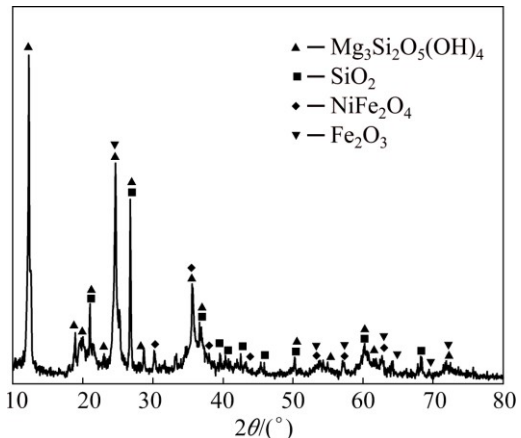


**Fig. 1** XRD pattern of nickel laterite ores

### 2.2 Experimental procedure

The ore samples pre-roasted at a desired temperature in a muffle furnace for 2 h were used for leaching silicon. The leaching experiments were performed in a 1 L round-bottom, Teflon, three-neck flask, which was fitted with a condenser, a mechanical stirrer and a plastic funnel for adding the samples. Firstly, a certain concentration of sodium hydroxide solution (800 mL) was poured into the flask, which was heated in a thermostatic oil bath at a stirring speed of 600 r/min. Once the temperature reached predetermined value, the desired amount of ore samples were added from the plastic funnel into the flask. At definite time intervals, 1 mL sample was withdrawn and immediately dissolved into 100 mL deionized water. The slurry was filtered to collect the liquid samples. The silicon concentration in liquid samples was measured by standard titration method.

The chemical compositions, mineralogical components, specific surface area, DTA/TG curves, and surface morphology of samples were detected using X-ray spectrometer (S-max, Rigaku), X-ray diffraction equipment (Rigaku-Ultima IV, Japan), BET surface area

analyzer (SSA-4300, Shanghai), thermal gravimetric analysis instrument (Diamond 6300, America) and scanning electron microscopy (Supra55, Germany), respectively.

### 3 Results and discussion

#### 3.1 Thermal analysis studies

Differential thermal analysis (DTA) and thermogravimetric analysis (TG) of low-grade nickel laterite ores were conducted from 0 to 1000 °C in air at a heating rate of 10 °C/min, and the results are presented in Fig. 2.

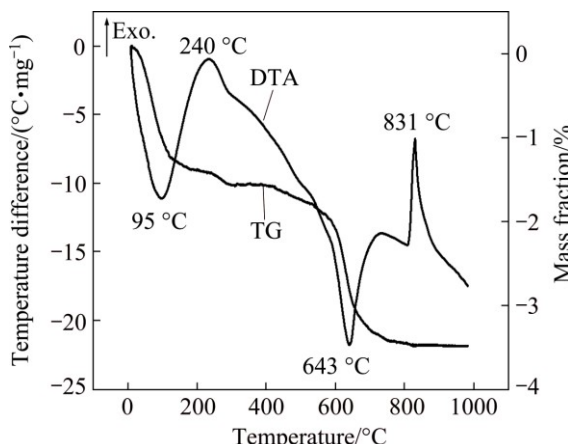


Fig. 2 DTA/TG curves of low-grade nickel laterite ores

It can be seen from DTA curve that there are two endothermic peaks at about 95 °C and 643 °C owing to the release of adsorbed water from laterite ores and the dehydroxylation of lizardite, respectively. Two large mass loss values presented by TG curve in different temperature ranges of 25–200 °C and 450–750 °C, corresponding to these two processes, are 1.41% and 1.77%, respectively.

On heating, also two exothermic peaks displayed from DTA at about 240 °C and 831 °C with relatively low mass loss are assigned to the oxidation of trevorite and the recrystallization of amorphous mineral, respectively [19].

Ore samples pre-roasted at different temperatures were detected by X-ray diffraction analyzer to figure out the roasted products, and the results are shown in Fig. 3.

As seen from XRD patterns in Fig. 3, the diffraction peak intensity of lizardite decreases as pre-roasting temperature increases. This can be attributed to the dehydroxylation of lizardite. When the pre-roasting temperature reaches 650 °C, the diffraction peaks of lizardite disappear, but the diffraction peaks of magnesium olivine ( $Mg_2SiO_4$ ) and protoenstatite ( $MgSiO_3$ ) emerge, which indicates that lizardite has decomposed almost completely. The results are corresponding to the endothermic peaks at 643 °C from

DTA curve in Fig. 2. The chemical reactions during pre-roasting can be written as follows:

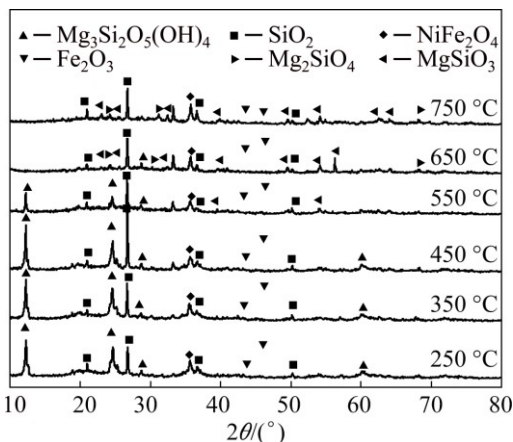
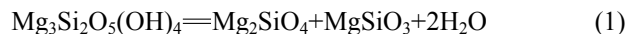


Fig. 3 XRD patterns of nickel laterite ores pre-roasted at different temperatures

#### 3.2 Pre-roasting of nickel laterite ores

The laterite ore samples pre-roasted at different temperatures ranging from 350 to 850 °C for 2 h were leached with sodium hydroxide solution for investigating the effects of pre-roasting temperatures on the extraction of silicon. The leaching conditions were fixed as follows: sodium hydroxide concentration of 60 g/L, solid/liquid ratio of 1:5, leaching time of 105 min, leaching temperature of 120 °C and particle size of 44–61 μm. The specific surface area of the ore samples pre-roasted at different temperatures was detected by a BET surface area analyzer. The variation of silicon extraction with pre-roasting temperature and specific surface area of ore samples is presented in Fig. 4.

As shown in Fig. 4, we can observe that the extraction of silicon increases rapidly from 30.3% to

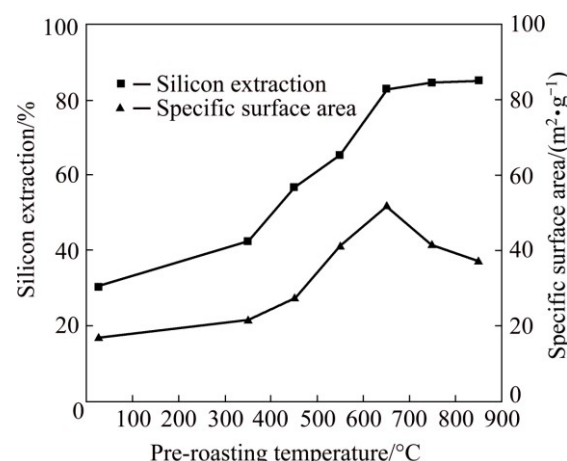


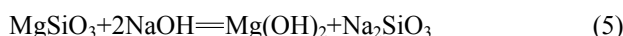
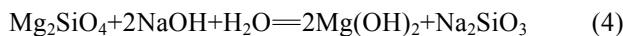
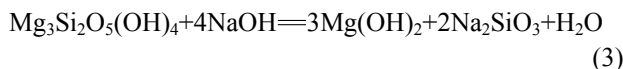
Fig. 4 Effect of pre-roasting temperature on silicon extraction and specific surface area

82.8% with pre-roasting temperature increasing from 25 to 650 °C. When the pre-roasting temperature is beyond 650 °C, the extraction of silicon almost keeps constant.

On the one hand, the rise of silicon extraction depends on the increase of ores' specific surface area. A large number of pores and fine particles of laterite ores can be obtained by pre-roasting to increase the specific surface area of ores. The numerical value of a sample without pre-roasting is 16.8 m<sup>2</sup>/g, which is increased to 51.59 m<sup>2</sup>/g after pre-roasting at 650 °C for 2 h, as presented in Fig. 4. Nevertheless, the specific surface area decreases due to the agglomeration of fine particles when pre-roasting temperature varies from 650 to 850 °C, the balance between the increase of temperature and the decrease of the specific surface area of the particles leads to the constant value of silicon extraction.

On the other hand, the increase of silicon extraction is closely related to the reaction activity of minerals. The dehydroxylation reaction of lizardite at 650 °C results in the destruction of crystal structure to form magnesium olivine ( $Mg_2SiO_4$ ) and protoenstatite ( $MgSiO_3$ ). They have higher reaction activity than lizardite because of their independent silicon oxygen anions. Thus, the pre-roasted temperature is chosen as 650 °C, and the ore samples pre-roasted at 650 °C for 2 h are used as the raw materials in the subsequent leaching experiments.

The main chemical reactions during the leaching process of ores can be typically represented as follows:



### 3.3 Leaching of nickel laterite ores

#### 3.3.1 Effect of leaching temperature

Under the condition of 60 g/L sodium hydroxide and solid/liquid ratio 1:5, the ores with 44–61 μm in size pre-roasted at 650 °C for 2 h were leached for 0–120 min at different temperatures (100–160 °C). The results from Fig. 5 show that the increase of leaching temperature effectively improves the extraction of silicon. At 100 °C, 75.89% silicon is extracted after 105 min, increasing to 89.86% at 160 °C. This is because increasing temperature can increase both chemical reaction rate and diffusion rate of reactants and products. In addition, a steadily rising trend of silicon extraction with leaching time can be seen from Fig. 5. After 15 min, a silicon extraction of 47.58% at 160 °C is achieved, and then goes up to 93.39% when the leaching time is 120 min. At the initial leaching stage, high sodium hydroxide concentration in the leaching system will accelerate

leaching reaction. With the increase of leaching time, sodium hydroxide concentration decreases and the silicon anion concentration increases gradually, thus the extraction of silicon rises slowly until equilibrium of system is reached finally.

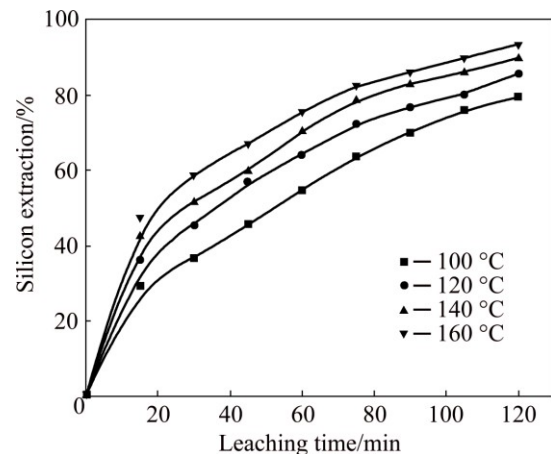


Fig. 5 Effect of leaching temperature on silicon extraction

#### 3.3.2 Effect of solid/liquid ratio

The influence of solid/liquid ratio on the extraction of silicon was studied in the range of 1:3–1:6 at 140 °C in 60 g/L of sodium hydroxide solution by using 44–61 μm of samples pre-roasted at 650 °C for 2 h, and the results are shown in Fig. 6. It can be seen that the extraction of silicon is improved gradually with the decrease of solid/liquid ratio. The silicon extraction can reach 72.33% and 89.42% after 120 min leaching at 1:3 and 1:6 solid/liquid ratio, respectively. It is well known that reaction rate  $R=kD_F^n$  where  $D_F=[Si]_{eq}-[Si]_t$  denotes the reaction driving force,  $[Si]_{eq}$  is the equilibrium concentration of Si and  $[Si]_t$  is the concentration of Si at time  $t$ . As solid/liquid ratio decreases,  $[Si]_t$  decreases and thus  $D_F$  increases, causing an increase of the reaction rate. It is obvious at the initial reaction stage where the initial reaction rate increases as the solid/liquid ratio decreases. However, the excess sodium hydroxide can significantly

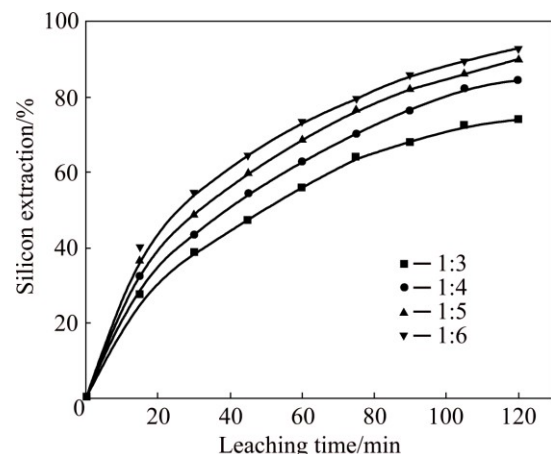
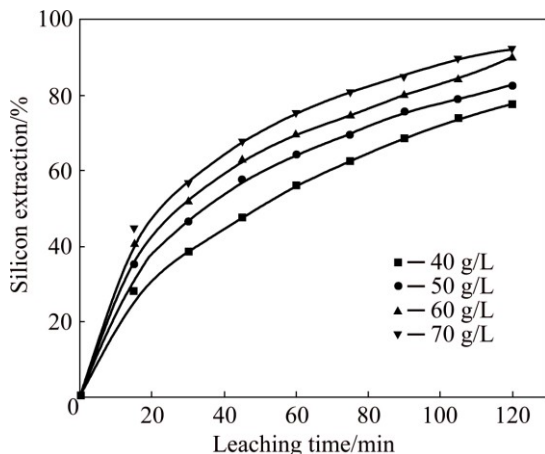


Fig. 6 Effect of solid/liquid ratio on silicon extraction

affect the economy of the whole process because of the complex recycling procedure [20]. Considering this fact, the solid/liquid ratio of 1:5 is considered to be appropriate.

### 3.3.3 Effect of sodium hydroxide concentration

The influence of sodium hydroxide initial concentration on the extraction of silicon was investigated by experiments conducted at 140 °C, 1:5 of solid/liquid ratio and 44–61 µm of samples pre-roasted at 650 °C for 2 h. The results in Fig. 7 show that the extraction of silicon increases from 77.48% to 92.11% after 120 min when the concentration of sodium hydroxide is increased from 40 to 70 g/L. This may be attributed to the fact that the increase of sodium hydroxide concentration causes the increase of the dissolution rate and dissolution degree of silicon, thereby increases silicon extraction.



**Fig. 7** Effect of sodium hydroxide concentration on silicon extraction

### 3.3.4 Effect of particle size

The ore samples at four different size fractions pre-roasted at 650 °C for 2 h were used as the raw materials in order to investigate the influence of sample particle size on the extraction of silicon. The leaching experiments were conducted at 140 °C while keeping solid/liquid ratio at 1:5 and sodium hydroxide concentration at 60 g/L. The results are presented in Fig. 8, where we can observe that the extraction of silicon increases from 75.5% to 89.89% with a decrease of particle size from 150–178 to 44–61 µm after 120 min of leaching time. This observation may be explained by the fact that the smaller the size of the particles is, the larger the contact area is, and the faster the reaction rate is. However, the ultrafine particles are difficult to obtain because of the technical limit and economic reasons [21].

### 3.3.5 Characterization of solid residues

The solid residues, obtained by roasting 44–61 µm of ore samples at 650 °C for 2 h and then leaching with 60 g/L of sodium hydroxide solution under the following

conditions: leaching temperature 140 °C, leaching time 120 min, stirring speed 600 r/min and solid/liquid ratio 1:5, were chosen for XRD, SEM and chemical analyses. The XRD pattern shown in Fig. 9 indicates that the major mineral phase of the solid residues is magnesium hydroxide ( $Mg(OH)_2$ ), hematite ( $Fe_2O_3$ ) and trevorite ( $NiFe_2O_4$ ). The main chemical reactions occur in the leaching process just as Eqs. (3)–(6) presented, while hematite and trevorite do not react with sodium hydroxide under the leaching conditions above.

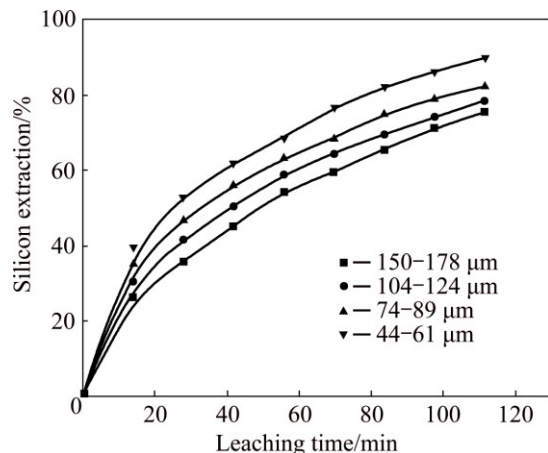


**Fig. 8** Effect of particle size on silicon extraction

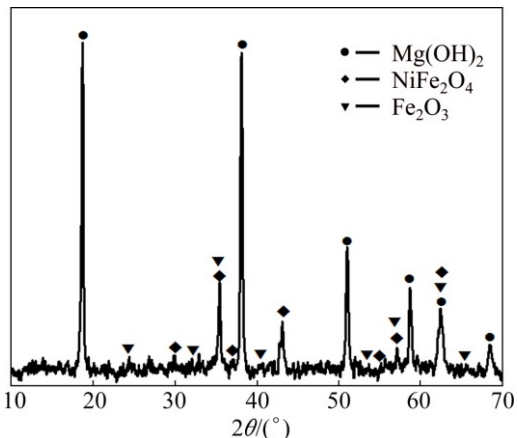


**Fig. 9** XRD pattern of solid residues

The chemical compositions of solid residues are shown in Table 2. Compared with Table 1, it can be seen that the contents of magnesium, iron and nickel elements are significantly increased, so the accumulation of other valuable elements by extracting silicon from nickel laterite ores can be achieved, which also create beneficial conditions for the recovery of valuable elements.

**Table 2** Main chemical compositions of solid residues (mass fraction, %)

MgO	$Fe_2O_3$	$Al_2O_3$	$SiO_2$	NiO	$Cr_2O_3$
27.65	42.62	6.74	5.64	1.78	0.61

The SEM images of ore samples and solid residues are presented in Fig. 10. It can be seen that the morphology of ore samples (Fig. 10(a)) is severely damaged due to the corrosion of sodium hydroxide and a large number of small particles eventually form and agglomerate together to become larger clusters after being leached at 140 °C for 120 min (Fig. 10(b)).

### 3.3.6 Kinetics analysis

The extraction of silicon from nickel laterite ores by sodium hydroxide solution leaching is a typical liquid–solid reaction, which could be analyzed with the shrinking core model [22,23]. According to this model, the reaction rate between solid particle and the reaction reagent may be controlled by one of the following steps:

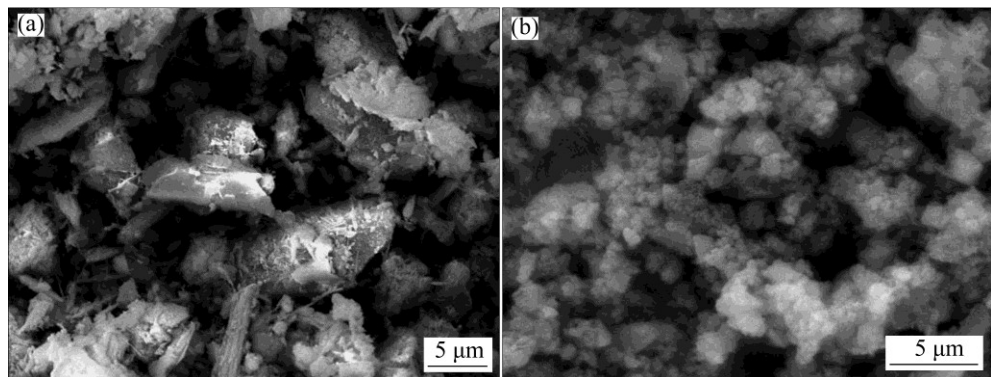


Fig. 10 SEM images of ore samples (a) and solid residues (b)

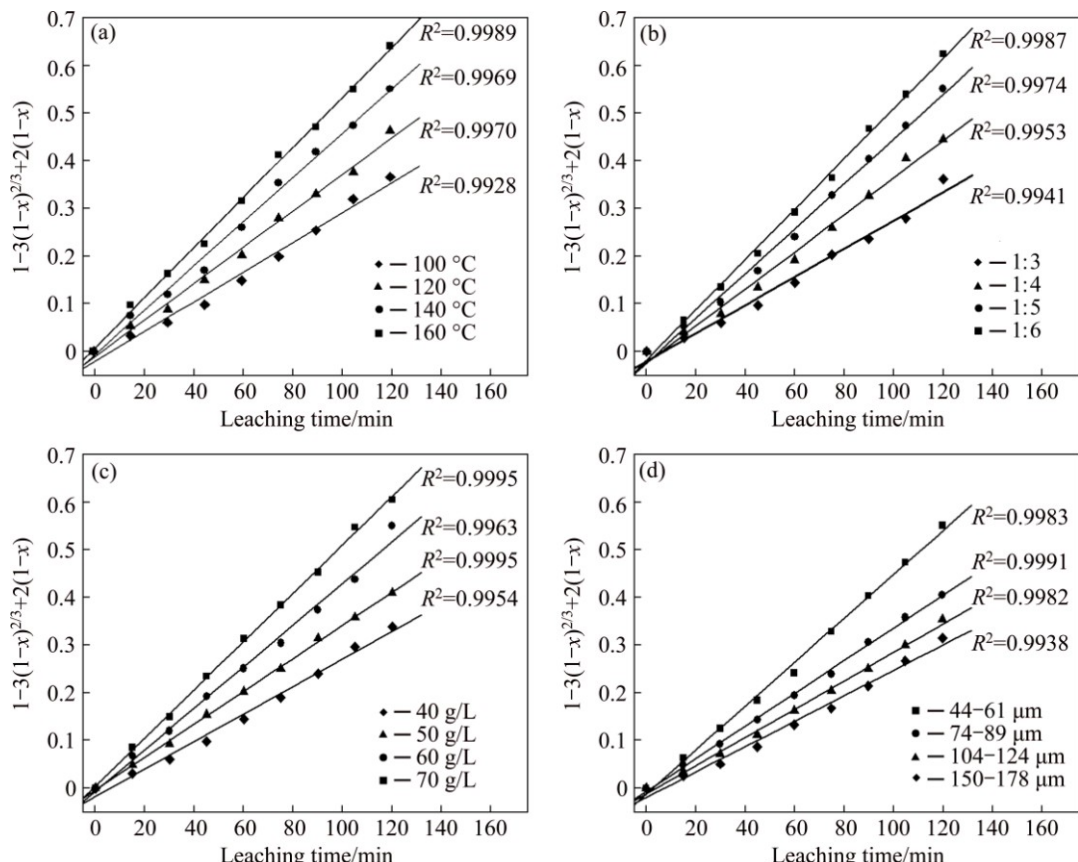


Fig. 11 Plots of  $1-3(1-x)^{2/3}+2(1-x)$  versus leaching time  $t$  at different leaching temperatures (a), solid/liquid ratios (b), sodium hydroxide concentrations (c) and particle sizes (d)

diffusion through the fluid film, diffusion through the product layer, or the chemical reaction on the surface. The integral rate equations for these models can be expressed as  $1-(1-x)^{2/3}=k_l t$ ,  $1-3(1-x)^{2/3}+2(1-x)=k_d t$ , and  $1-(1-x)^{1/3}=k_r t$ , respectively [24–27], where  $x$  is the extraction of silicon,  $k_l$  is the apparent rate constant for diffusion through the fluid film,  $k_d$  is the pore diffusion rate constant,  $k_r$  is the apparent rate constant for the surface chemical reaction and  $t$  is the leaching time.

It can be found that the best linear relationship is obtained from the equation  $1-3(1-x)^{2/3}+2(1-x)=k_d t$  after the experimental data collected at different temperatures are evaluated by the shrinking core model, as shown in Fig. 11(a).

Furthermore, the linear relation between  $1-3(1-x)^{2/3}+2(1-x)$  and  $t$  can also be seen in Figs. 11(b)–(d) for solid/liquid ratio, sodium hydroxide concentration and particle size, respectively. In accordance with these results, the equation representing the kinetics of this process is determined to obey the diffusion through the product layer.

In addition, if the diffusion through the product layer controls the reaction rate, the relation between the apparent rate constant and the inverse of the square of particle radius must be linear. This relationship is given in Fig. 12. Figure 12 confirms that the diffusion through the product layer model can be the rate controlling step for the leaching process of nickel laterite ores.

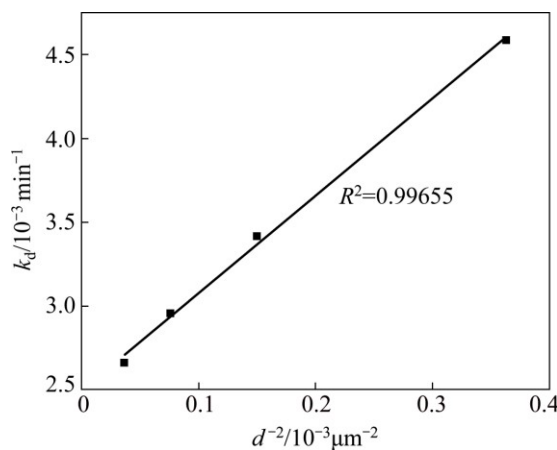


Fig. 12 Plot of  $k_d$  versus  $d^{-2}$  for different particle sizes

The apparent rate constants determined from Fig. 11(a) are plotted according to the Arrhenius equation,  $k_d=k_0\exp[-E_a/(RT)]$  as shown in Fig. 13. Using the Arrhenius equation, the apparent activation energy and the rate constant are calculated as 11.63 kJ/mol and  $13.53\times 10^{-2}\text{ min}^{-1}$ , respectively. After the evaluation of activation energy and pre-exponential factor, the kinetics model for the leaching process of nickel laterite ores can

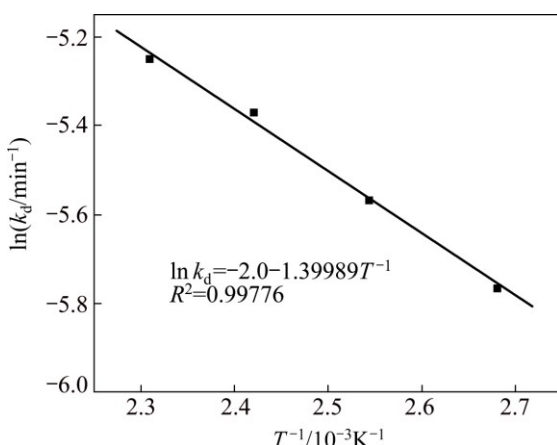


Fig. 13 Arrhenius plot for extracting silicon from nickel laterite ores

be expressed as  $1-3(1-x)^{2/3}+2(1-x)=13.53\times 10^{-2}\times \exp[-11.63/(RT)]t$ .

## 4 Conclusions

1) The reaction activity of nickel ores in alkaline solution can be effectively improved by pre-roasting at 650 °C for 2 h, which can be attributed to the formation of high reactive minerals including magnesium olivine and protoenstatite from the dehydroxylation of lizardite, and the increase of ores' specific surface area.

2) The extraction of silicon increased with increasing leaching temperature, leaching time and sodium hydroxide concentration, but decreased with increasing solid/liquid ratio and particle size. It is estimated that 89.89% silicon could be extracted when ore samples (44–61 μm) were pre-roasted at 650 °C for 2 h firstly, and then reacted with sodium hydroxide solution (60 g/L) with a solid/liquid ratio of 1:5 at 140 °C for 120 min, the other elements such as magnesium, iron and nickel were accumulated in the solid residues.

3) The kinetic study indicates that the leaching process of nickel laterite ores is controlled by the diffusion through the product layer. The activation energy was calculated to be 11.63 kJ/mol and the kinetics equation can be expressed as  $1-3(1-x)^{2/3}+2(1-x)=13.53\times 10^{-2}\exp[-11.63/(RT)]t$ .

## References

- [1] PICKLES C A. Microwave heating behaviour of nickeliferous limonitic laterite ores [J]. Minerals Engineering, 2004, 17(6): 775–784.
- [2] LEE H Y, KIM S G, OH J K. Electrochemical leaching of nickel from low-grade laterites [J]. Hydrometallurgy, 2005, 77(3–4): 263–268.
- [3] DALVI A D, BACON W G, OSBORNE R C. The past and the future of nickel laterites [C]//Proceedings of PDAC 2004 International Convention. Toronto: The Prospectors and Developers Association of Canada, 2004: 1–27.
- [4] MUDD G M. Global trends and environmental issues in nickel mining: Sulfides versus laterites [J]. Ore Geology Reviews, 2010, 38(1–2): 9–26.
- [5] NOSRATI A, QUAST K, XU D F, SKINNER W, ROBINSON D, ADDAI-MENSAH J. Agglomeration and column leaching behaviour of nickel laterite ores: Effect of ore mineralogy and particle size distribution [J]. Hydrometallurgy, 2014, 146(3): 29–39.
- [6] PICKLES C A. Drying kinetics of nickeliferous limonitic laterite ores [J]. Minerals Engineering, 2003, 16(12): 1327–1338.
- [7] SOLER J M, CAMA J, GALÍ S, MELÉNDEZ W, RAMÍREZ A, ESTANGA J. Composition and dissolution kinetics of garnierite from the Loma de Hierro Ni-laterite deposit, Venezuela [J]. Chemical Geology, 2008, 249(1): 191–202.
- [8] ZHU De-qing, CUI Yu, HAPUGODA S, VINING K, PAN Jin. Mineralogy and crystal chemistry of a low grade nickel laterite ore [J]. Transactions of Nonferrous Metals Society of China, 2012, 22(4): 907–916.

- [9] NORGATE T, JAHANSNAH S. Assessing the energy and greenhouse gas footprints of nickel laterite processing [J]. Minerals Engineering, 2011, 24(7): 698–707.
- [10] SWAMY Y V, KAR B, MOHANTY J K. Physico-chemical characterization and sulphatization roasting of low-grade nickeliferous laterites [J]. Hydrometallurgy, 2003, 69(1–3): 89–98.
- [11] LU J, LIU S J, JU S G, DU W G, PAN F, YANG S. The effect of sodium sulphate on the hydrogen reduction process of nickel laterite ore [J]. Minerals Engineering, 2013, 49(8): 154–164.
- [12] HALLBERG K B, GRAIL B M, PLESIS C A D, JOHNSON D B. Reductive dissolution of ferric iron minerals: A new approach for bio-processing nickel laterites [J]. Minerals Engineering, 2011, 24(7): 620–624.
- [13] MACCARTHY J, ADDAI-MENSAH J, NOSRATIA. Atmospheric acid leaching of siliceous goethitic Ni laterite ore: Effect of solid loading and temperature [J]. Minerals Engineering, 2014, 69: 154–164.
- [14] WILLS B A, NAPIER-MUNN T. Will's mineral processing technology: An introduction to the practical aspects of ore treatment and mineral recovery [M]. 7th ed. Amsterdam: Elsevier, 2006.
- [15] MCDONALD R G, WHITTINGTON B I. Atmospheric acid leaching of nickel laterites review: Part I. Sulphuric acid technologies [J]. Hydrometallurgy, 2008, 91(1): 35–55.
- [16] LIU K, CHEN Q Y, HU H P, YIN Z L, WU B K. Pressure acid leaching of a Chinese laterite ore containing mainly maghemite and magnetite [J]. Hydrometallurgy, 2010, 104(1): 32–38.
- [17] ZHAI Yu-chun, MU Wen-ning. A green process for recovering nickel from nickeliferous laterite ores [J]. Transactions of Nonferrous Metals Society of China, 2010, 20(S2): s65–s70.
- [18] MU Wen-ning, ZHAI Yu-chun. Dissolution kinetics of nickeliferous laterite ore in molten sodium hydroxide system [J]. Transactions of Nonferrous Metals Society of China, 2010, 20(2): 330–335.
- [19] TARTAJ P, CERPA A, GARĆIA-GONZALEZ, M T, SERNA C J. Surface instability of serpentine in aqueous suspensions [J]. Journal of Colloid & Interface Science, 2000, 231(1): 176–181.
- [20] GLEESON S A, HERRINGTON R J, DURANGO J, VELÁZQUEZ C A, KOLL G. The mineralogy and geochemistry of the Cerro Matoso S. A. Ni laterite deposit, Montelíbano, Colombia [J]. Economic Geology, 2004, 99(6): 1197–1213.
- [21] KAYA S, TOPKAYA Y A. High pressure acid leaching of a refractory lateritic nickel ore [J]. Minerals Engineering, 2011, 24(11): 1188–1197.
- [22] LEVENSPIEL O. Chemical reaction engineering [M]. 3rd ed. New York: Willey, 1999.
- [23] YANG Sheng-hai, LI Hao, SUN Yan-wei, CHEN Yong-ming, TANG Chao-bo, HE Jing. Leaching kinetics of zinc silicate in ammonium chloride solution [J]. Transactions of Nonferrous Metals Society of China, 2016, 26(6): 1688–1695.
- [24] ZHU Xiao-bo, LI Wang, GUAN Xue-mao. Kinetics of titanium leaching with citric acid in sulfuric acid from red mud [J]. Transactions of Nonferrous Metals Society of China, 2015, 25(9): 3139–3145.
- [25] WEN C Y. Non-catalytic heterogeneous solid-fluid reaction models [J]. Industrial & Engineering Chemistry, 1968, 60(9): 34–52.
- [26] YANG Z, LI H Y, YIN X C, YAN Z M, YAN X M, XIE B. Leaching kinetics of calcification roasted vanadium slag with high CaO content by sulfuric acid [J]. International Journal of Mineral Processing, 2014, 133: 105–111.
- [27] KAVCI E, ÇALBAN T, ÇOLAK S, KUŞLU S. Leaching kinetics of ulexite in sodium hydrogen sulphate solutions [J]. Journal of Industrial and Engineering Chemistry, 2014, 20(5): 2625–2631.

## 低品位红土镍矿预焙烧-碱浸过程中 硅的转化和浸出动力学

牟文宁<sup>1,2</sup>, 陆修远<sup>1</sup>, 崔富晖<sup>3</sup>, 罗绍华<sup>1,2</sup>, 翟玉春<sup>3</sup>

1. 东北大学 秦皇岛分校 资源与材料学院, 秦皇岛 066004;
2. 秦皇岛市资源清洁转化与高效利用重点实验室, 秦皇岛 066004;
3. 东北大学 冶金学院, 沈阳 110819

**摘要:** 研究低品位红土镍矿预焙烧过程矿相的转化和碱浸过程硅的提取。结果表明, 红土镍矿经 650 °C 预焙烧 2 h, 由于利蛇纹石转化为镁橄榄石和原顽辉石使得矿物的活性显著提高, 当磨细矿样(44~61 μm)经预焙烧后, 与氢氧化钠溶液(60 g/L)按照 1:5 的固液比混合在 140 °C 浸出 120 min, 硅的提取率可达到 89.89%, 镁、铁、镍等有价元素在固体渣中得到富集。红土镍矿的浸出动力学可由扩散通过产物层控制模型来描述, 计算得到过程的活化能为 11.63 kJ/mol, 动力学方程为  $1-3(1-x)^{2/3}+2(1-x)=13.53 \times 10^{-2} \exp[-11.63/(RT)]t$ 。

**关键词:** 低品位红土镍矿; 提硅; 矿相转化; 碱浸动力学

(Edited by Wei-ping CHEN)